Encapsulation of resveratrol using food-grade concentrated double emulsions: emulsion characterization and rheological behaviour

María Matos, Gemma Gutiérrez, Lemuel Martínez-Rey, Olvido Iglesias, and Carmen Pazos*

Department of Chemical and Environmental Engineering, University of Oviedo, Julián Clavería 8, 33006 Oviedo, Spain.

*Corresponding autor: Tel: +34 985103509; Fax: +34 985103434

E-mail addresses: matosmaria@uniovi.es (María Matos), gutierrezgemma@uniovi.es (Gemma Gutiérrez), UO223873@uniovi.es (Lemuel Martínez-Rey), oih@uniovi.es (Olvido Iglesias), cpazos@uniovi.es (Carmen Pazos)

Abstract

The aim of this work was to prepare concentrated water-in-oil-in-water ($W_1/O/W_2$) double emulsions to entrap resveratrol (RSV) with high encapsulation efficiency, good stability, and appropriate rheological behaviour.

W_1/O was formulated with an ethanol/water RSV solution (W_1) dispersed in Miglyol 812 (O) (20 vol.%) with polyglycerol polyricinoleate as stabiliser. W_2 was a 2% w/v Tween 20 solution with and without sodium carboximethylcellulose as thickening agent. Different volumetric ratios (20/80 to 80/20) of W_1/O dispersed into W_2 were used.

$W_1/O/W_2$ emulsions were characterized in terms of visual inspection, droplet size distribution, and stability. The rheology of these double emulsions was fully studied.

Actual encapsulation efficiency was determined considering the non-encapsulated RSV recovery yield.

The concentrated $W_1/O/W_2$ double emulsions with the optimum formulation showed high encapsulation efficiency (up to 58%), good storage stability, shear-thinning behaviour, and dominant elastic character, with 6.2 mg/L of encapsulated RSV. These double emulsions may be suitable for food applications.

Keywords: resveratrol, double emulsion, concentrated emulsion, encapsulation efficiency

Abbreviations: BS, backscattering profile; CMC, sodium carboximethylcellulose; EE, encapsulation efficiency; HIPE, high internal phase emulsion; HLB, hydrophilic-lipophilic balance; O, oil phase; PGPR, polyglycerol polyricinoleate; RP-HPLC, reversed-phase high-performance liquid chromatography; RSV, resveratrol; TS, transmission profile; UV-vis, ultraviolet-visible; W_1, inner aqueous phase; W_2, external aqueous phase; W_1/O, primary emulsion; $W_1/O/W_2$, water-in-oil-in-water double emulsion.

1. Introduction

Resveratrol (3,5,4'-trihydroxystilbene, RSV) is a natural polyphenol present in many plants. Therefore, RSV can be got from different sources, such as grapes, nuts, berries, dark chocolate, and especially red wine, where the highest RSV concentration is found (Guerrero et al., 2009; Mullin, 2011).

Many in vitro and in vivo studies have suggested that RSV has a great number of potential health benefits in combating diseases, such as cancer, diabetes, neurodegeneration, cardiovascular disorders, inflammation, and other age-related pathologies (Diaz-Gerevini et al., 2016; Murtaza et al., 2013; Novelle et al., 2015; Saiko et al., 2008; Yang et al., 2014).

However, this great RSV potential is hindered by its poor pharmacokinetic properties, such as low aqueous solubility, low photostability, short biological half-life, and rapid metabolism and elimination (Amri et al., 2012; Francioso et al., 2014; Gomes-Silva et al., 2013; Neves et al., 2012; Yang et al., 2015). To overcome these limitations, encapsulation of RSV seems to be a good alternative for using this valuable ingredient in food, pharmaceutical and cosmetic industries.

Several encapsulation studies have been conducted to protect RSV from degradation, increasing its solubility in water and improving its chemical stability and bioavailability via multiparticulate forms and colloidal carriers (Amri et al., 2012; Davidov-Pardo & McClements, 2014; Ganesan & Choi, 2016; Pangeni et al., 2014; Sessa et al., 2014; Soo et al., 2016; Summerlin et al., 2015).

Double emulsions, such as water-in-oil-in-water ($W_1/O/W_2$) emulsions, are one of these colloidal delivery systems available to encapsulate and protect RSV (Hemar et al., 2010; Matos et al., 2014; Wang et al., 2017).

$W_1/O/W_2$ double emulsions consist of small water droplets trapped within larger oil droplets that are themselves dispersed in a continuous water phase (Aserin, 2008; Kim et al., 2003; McClements & Li, 2010; Muschiolik, 2007).

One of the main drawbacks of $W_1/O/W_2$ double emulsions is their low stability, due to the excess free energy associated with droplets surface of the primary and secondary emulsions. The stability of the W_1/O primary emulsion must be ensured to obtain a stable $W_1/O/W_2$ double emulsion, which depends on droplet sizes, amounts of dispersed and continuous phase, and emulsifier affinity for both phases (Garti, 1997; Muschiolik & Dickinson, 2017; Schuch et al., 2013; Yildrim et al., 2017).

Although $W_1/O/W_2$ double emulsions have shown their suitability to encapsulate RSV, encapsulation efficiencies (EE) were not as high as those for other types of colloidal systems (Matos et al., 2014), even when it was enhanced by membrane emulsification techniques (Matos et al., 2015a). Also, the concentration of encapsulated RSV in the final double emulsion should be clearly improved regarding previous works. Wang et al. (2017) reported high EE values but with very low RSV concentration, and Hemar et al. (2010) used an initial RSV concentration larger than the RSV solubility in the W_1 phase, what means that RSV was not completely dissolved under those conditions.

On the other hand, high internal phase emulsions (HIPEs) are concentrated systems with a large volume of internal (or dispersed) phase. HIPEs contain more than 74 vol.% of internal phase, which corresponds to the Ostwald critical volume. But it is possible to reach higher packing values by the concentration of polydisperse emulsions, since small droplets may fill the voids between the large ones even losing their spherical shape becoming polyhedral (Babak & Stebe, 2002; Cameron & Sherrington, 1996). These systems have wide application in cosmetics, foodstuffs, emulsion explosives, drug delivery systems, reaction media, and especially in the production of porous polymers (emulsion-templated porous polymers, PolyHIPEs) (Llinàs et al., 2013; Park et al., 2003; Silverstein, 2014; Solans et al., 2003; Zhang & Guo, 2017).

Moreover, stability studies revealed that HIPEs are very stable against destabilization phenomena and lead to high EE values (Gutiérrez et al., 2014; Matos et al., 2015b).

In addition to that, a few studies with new approaches to produce concentrated double emulsions have been recently published (Leal-Calderon et al., 2012; Lei et al., 2016; Li et al., 2014).

In this paper, the preparation of concentrated $W_1/O/W_2$ double emulsions containing RSV through a two-step mechanical emulsification process is reported. The main purpose of this work was to prepare a product with high RSV content and to enhance the EE through the use of concentrated $W_1/O/W_2$ double emulsions with large stability. In previously reported works using double emulsions to encapsulate RSV, the RSV EE values were low (Matos et al., 2014; Matos et al., 2015a), or the final RSV concentration in the double emulsion was small (Wang et al., 2017), or the RSV concentration in W_1 was higher than its solubility limit, what indicated the presence of a suspension instead of a solution (Hemar et al., 2010).

Moreover, it is well known that the determination of EE in double emulsions requires the emulsion destabilization (frequently by centrifugation) and subsequent extraction of a sample of W_2 previously filtered to analyse the non-encapsulated RSV (Hemar et al., 2010; Wang et al., 2017). However, with this experimental procedure some amount of non-encapsulated RSV could remain retained either by interactions with filter materials or with other formulation components, which would be considered as encapsulated RSV providing an overestimated EE value. In this work, therefore, the RSV amount lost during centrifugation, filtration, and W_2 sample extraction processes was measured and taken into consideration for determining the actual EE value.

Furthermore, the rheology of these double emulsions was fully studied since it is largely influenced by the emulsion concentration and the emulsion rheological behaviour is also a key parameter in the final application of the product (Pal, 2011).

2. Materials and methods

2.1. Materials

RSV ($C_{14}H_{12}O_3$), absolute ethanol, Tween® 20 (polyoxyethylenesorbitan monolaurate, $C_{58}H_{114}O_{26}$), and sodium carboximethylcellulose (CMC, $C_8H_{16}NaO_8$) with polymerization degree 1100 (molar mass=982 kg/kmol) were purchased from Sigma Aldrich (USA). Miglyol® 812 (density 945 kg/m^3 at 20 ºC), which is a neutral oil formed by esters of caprylic and capric fatty acids and glycerol, was supplied by Sasol GmbH (Germany). Polyglycerol polyricinoleate (PGPR, $C_{21}H_{42}O_6$) was obtained from Brenntag AG (Germany). Sodium chloride was supplied by Panreac (Spain).

The hydrophilic-lipophilic balance (HLB) values of the emulsifiers tested in this study are: Tween 20=16.7; PGPR=3.0.

HPLC-grade methanol, acetonitrile, 2-propanol, and acetic acid were obtained from Sigma Aldrich (USA).

Paraffin oil supplied by VWR International (USA) was used as dispersant for droplet size measurements of W_1/O emulsions.

2.2. W_1/O emulsion preparation

The primary W_1/O emulsion was formulated with 20 vol.% of inner aqueous phase (W_1) and 80 vol.% of oil phase (O).

Miglyol 812 containing 5 wt.% of the hydrophobic emulsifier (PGPR) previously dissolved by magnetic stirring at 50°C for 30 min was used as the oil phase. PGPR is highly effective for stabilizing W/O emulsions (Márquez et al., 2010; Wolf et al., 2013).

In order to increase RSV solubility, a 20 vol.% ethanol/water solution with 50 mg/L of RSV was selected as the inner aqueous phase.

0.1M NaCl was added to the inner aqueous phase in all double emulsions to ensure W_1 droplets stability because it had been previously reported that electrolytes increase W_1/O emulsion stability (Jiang et al., 2013; Márquez et al., 2010).

Both phases were emulsified in glass vessels by high shear mixing (Silentcruser M Homogenizer, Heidolph, Germany) using a 6 mm dispersing tool at 15,000 rpm for 10 min.

2.3. W_1/O/W_2 double emulsions preparation

The W_1/O/W_2 double emulsions were prepared dispersing the W_1/O primary emulsion into the external aqueous phase (W_2) at several volumetric ratios of W_1/O in W_2: 20/80, 40/60, 50/50, 60/40, 70/30, and 80/20. W_2 was a 2% (w/v) Tween 20 solution. Emulsification was carried out by mixing the continuous and dispersed phases with the aforementioned Silentcruser M Homogenizer at 5,000 rpm for 2 min.

These double emulsions were also formulated with 0.5% (w/v) CMC in the W_2 phase. Overnight magnetic stirring was needed to completely dissolve CMC. Then, 2% (w/v) Tween 20 was added and dissolved proceeding with the stirring for 30 min.

0.1M NaCl was also added to the W_2 phase to maintain an appropriate osmotic balance between W_1 and W_2, the inner and outer aqueous phases, in all emulsions.

2.4. Emulsion characterization

2.4.1. Droplet size and visual inspection

Emulsion droplet size distributions were analysed using laser light scattering technique in a Mastersizer S long bench apparatus (Malvern Instruments, Ltd. UK).

For single W_1/O emulsion measurements, the samples were dispersed in paraffin oil, whereas $W_1/O/W_2$ double emulsion samples were diluted with deionized water.

Micrographs of the emulsions were obtained with a light microscope Olympus BX50 (Olympus, Japan) with 10-100x magnification using UV-vis and fluorescence lamps.

2.4.2. Resveratrol analysis and encapsulation efficiency

RSV content in the external aqueous phases was determined by RP-HPLC (HP series 1100 chromatograph, Hewlett Packard, USA). The system was equipped with a UV-vis absorbance detector HP G1315A or a fluorescence detector 1260 Infinity A (Agilent Technologies, USA). The separation was performed with a reversed phase column Zorbax Eclipse Plus C_{18} of 5 μm particle size and 4.6 mm × 150 mm (Agilent Technologies, USA).

The mobile phase consisted of a mixture of (A) 100% milliQ-water and (B) 100% methanol with gradient elution at a flow rate of 0.8 mL/min. The step gradient started with 80% mobile phase (A) running 100% of mobile phase (B) in minute 5 for 10 min. The mobile phase (B) was run for 2 min after each injection to prepare the column for the next run. The separation was carried out at room temperature. A wavelength of 305 nm was used for UV-vis detector while fluorescence detector was used at $\lambda_{excitation}/\lambda_{emission}$ of 310/410 nm. The column was cleaned after each analysis by running first the mobile phase (A) for 20 min and a mobile phase (C) consisting of 50% acetonitrile, 25% milliQ-water, 25% 2-propanol, and 0.01% acid acetic for 40 min at a flow rate of 0.25 mL/min. Finally, the column was rinsed with 50% of mobile phase (A) and 50% of mobile phase (B) for another 20 min.

The external aqueous phases injected in the HPLC were previously recovered by centrifugation at low speed (1000 rpm for 20 min) followed by filtration with a 0.22 μm polyvinylidene difluoride syringe filter to remove all the oil phase that could be still present (Matos et al., 2014, 2015a).

The recovery yield (R_y) after the centrifugation and filtration stages was used to know the amount of RSV retained during both separation processes. This amount corresponded to non-encapsulated RSV either retained by interactions with filter materials or with other formulation components, which could be considered as encapsulated RSV providing an overestimated EE value.

For this purpose, a standard emulsion, where 100% of W_1 is present in W_2, was required. Therefore, an oil-in-water (O/W_2) emulsion was prepared using the same formulation as in the other experiments. This O/W_2 emulsion was then diluted at the same ratio with W_1, which contained the appropriate amount of RSV initially added. Then, the concentration in the recovered aqueous phases ($C_{recovered}$) was determined by RP-HPLC. A blank without RSV that consisted of an O/W_2 emulsion diluted with W_1 was prepared for performing this analysis. The recovery yield, R_y, was calculated as:

$$R_y = \frac{C_{recovered} \times 100}{C_0} \qquad (1)$$

where C_0 is the maximum concentration expected in the external aqueous phase.

EE of these double emulsions was defined as the percentage of encapsulated RSV in W_1 that remained in the W_1/O primary emulsion after the second emulsification step (Matos et al., 2014, 2015a; O´Regan & Mulivhill, 2009). It was calculated as:

$$EE = 100 - \frac{C_{recovered} \times 100}{C_0 R_y} \qquad (2)$$

Three to five replicates of the analytical measurements were conducted for each sample and the average value was taken.

2.4.3. Stability

Emulsion stability was determined by measuring backscattering (BS) and transmission (TS) profiles in a Turbiscan apparatus (Formulaction, France). Samples of emulsions were placed without dilution in the test cells. Transmitted and backscattered light was monitored as a function of time and cell height for 9 days at 30 °C.

2.4.4. Rheology

A Haake MARS II rotational rheometer (Thermo Fisher Scientific, USA) in combination with a serrated plate-plate configuration (PP35) was used for emulsion rheological measurements performed at 25 °C. The measuring gap was 1 mm. Emulsion samples were deposited on the rheometer plate for 5 min before making measurements to minimize any internal stress. All measurements were replicated twice, and they were performed during the next 24 h after emulsion preparation to avoid aging effects.

2.4.4.1. Steady-state flow measurements

Viscosities of the double emulsions were determined at 25 °C using a linear ramp of shear rates increasing from 1 to 500 s^{-1} in 5 min.

2.4.4.2. Oscillatory rheological analyses

Frequency sweep tests were carried out from 0.1 to 10 Hz at a constant shear stress of 1 Pa and 25°C.

3. Results and discussion

3.1. Droplet size distributions

Fig. 1A shows the droplet size distribution of the primary emulsion W_1/O, whose D(*v*,0.5) value was 0.66±0.14 μm. A peak is also observed around 0.2 μm likely caused by the presence of PGPR (inverse) micelles, as it was already reported (Matos et al., 2015a).

As Figs. 1B-1C show, droplet size distributions of the $W_1/O/W_2$ double emulsions prepared at several volumetric ratios of the W_1/O primary emulsion in the W_2 external aqueous phase are bimodal and highly polydisperse. The mean peak for all these double emulsions is in the 10-30 μm range, and this value is consistent with those of previous studies (Hemar et al., 2010; Matos et al., 2014, 2015a).

It was not possible to prepare an 80/20 volumetric ratio double emulsion with CMC in its external aqueous phase since emulsion inversion took place.

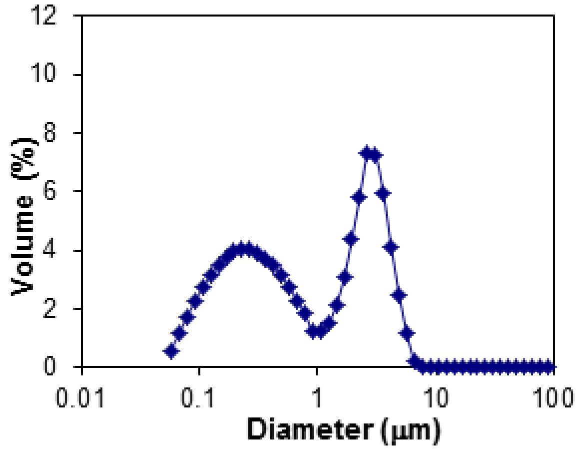

(A)

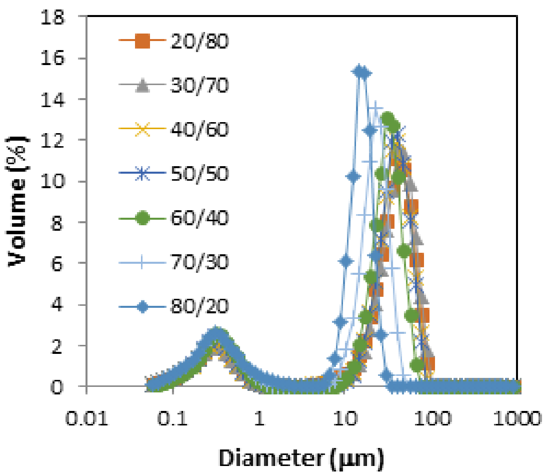

(B)

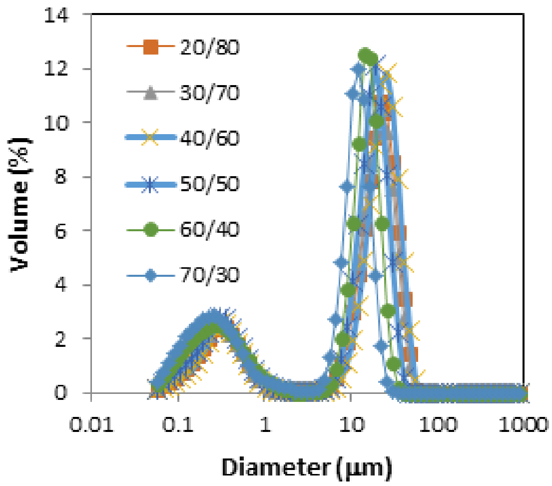

(C)

Fig. 1. Droplet size distributions of the W_1O primary emulsion (A) and the $W_1/O/W_2$ double emulsions formulated at several volumetric ratios of W_1/O in W_2 without (B) and with (C) 0.5% (w/v) of CMC in the external aqueous phase

As can be seen, there are no significant differences in size due to the presence (Fig. 1C) or absence (Fig. 1B) of CMC. It is only noticed a decrease in the mean size for concentrated double emulsions at volumetric ratios of 70/30 and 80/20 probably due to the proximity to the emulsion inversion point (Rondón-González et al., 2006).

3.2. Visual inspection

Fig. 2 shows some of the optical microscopy images of $W_1/O/W_2$ double emulsions formulated with and without CMC in W_2. Only photomicrographs for the most representative volumetric ratios are given in Fig. 2, and they show experimental results that are in good agreement with the mean droplet sizes provided by the Mastersizer equipment.

The presence of inner water droplets can be observed in all images, and also how the W_1/O droplets start to be more packed as the volumetric ratio of W_1/O in W_2 increases.

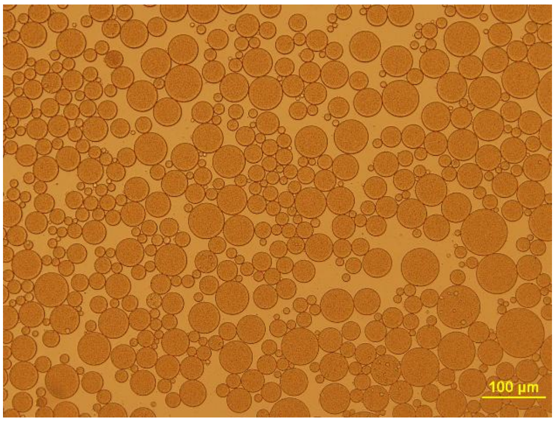

30/70 without CMC in W_2

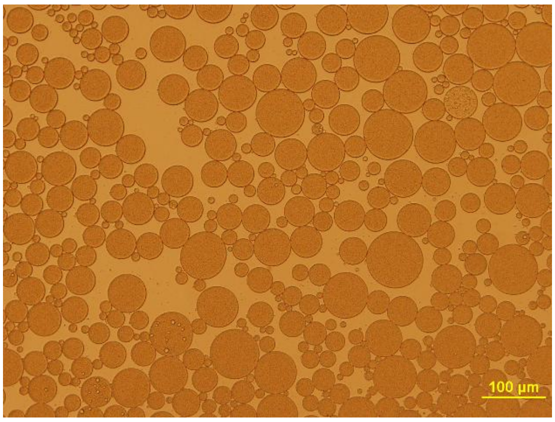

30/70 with CMC in W_2

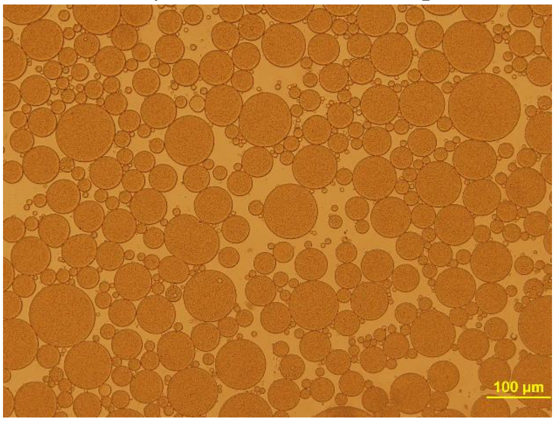

50/50 without CMC in W_2

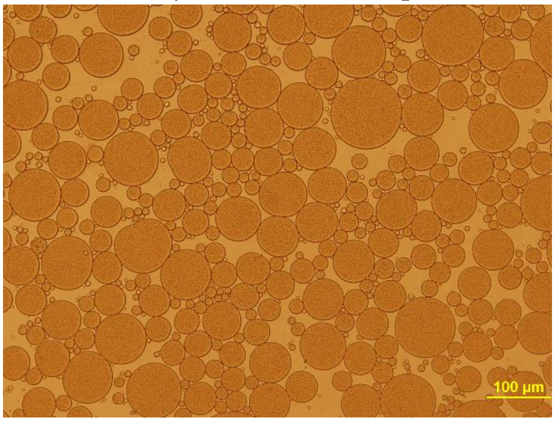

50/50 with CMC in W_2

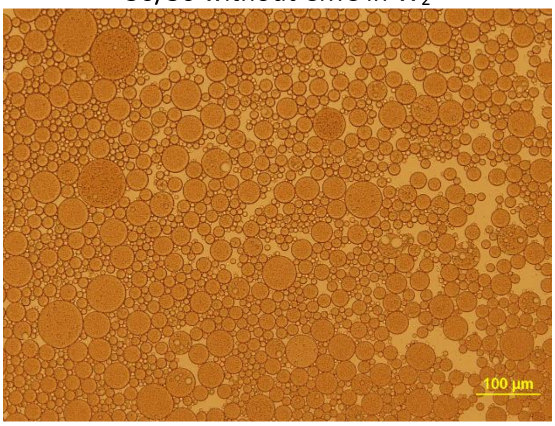

70/30 without CMC in W_2

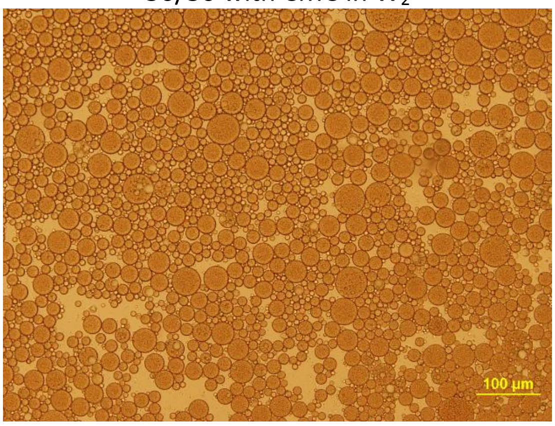

70/30 with CMC in W_2

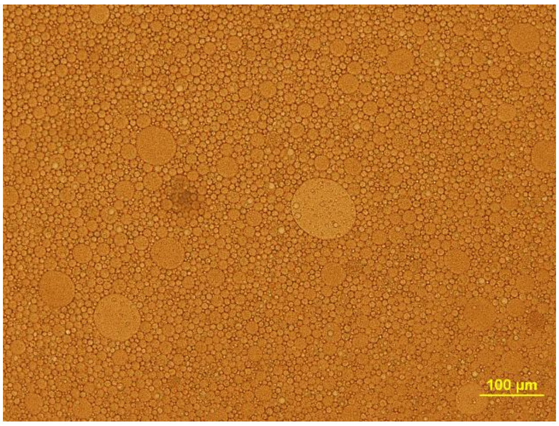

80/20 without CMC in W_2

Fig. 2. Optical microscopy images of $W_1/O/W_2$ double emulsions formulated without and with 0.5% (w/v) of CMC in W_2 at several volumetric ratios of W_1/O in W_2

3.3. Encapsulation efficiency

EE values for $W_1/O/W_2$ double emulsions formulated at several volumetric ratios of W_1/O in W_2 are depicted in Fig. 3.

It is observed that EE remains nearly constant up to a 60/40 volumetric ratio of W_1/O in W_2 for all double emulsions independently if CMC is or not present in W_2.

For volumetric ratios higher than 60/40, the EE values greatly increase with this ratio for both types of emulsion. The maximum EE value (58.3%) is achieved when the double emulsion turns into a HIPE.

In all cases, double emulsions with CMC show EE values slightly higher than those for double emulsions without CMC in the external aqueous phase.

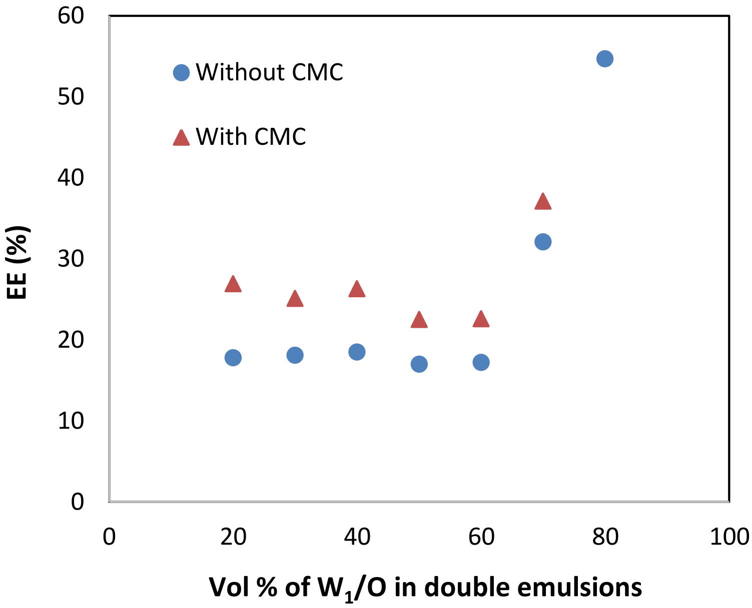

Fig. 3. Encapsulation efficiency of RSV for $W_1/O/W_2$ double emulsions formulated without and with 0.5% (w/v) of CMC in the external aqueous phase at several volumetric ratios of W_1/O in W_2

Table 1 shows, in a comparative way, the results from this study and from previous works where RSV was also encapsulated using $W_1/O/W_2$ double emulsions (Hemar et al., 2010; Matos et al., 2015a; Wang et al., 2017). It is important to point out that we take into account the R_y of RSV for the calculation of its EE. This procedure enables us to measure the amount of non-encapsulated RSV retained during both separation processes (centrifugation and filtration) and to avoid an EE overestimation. For that reason, our EE values in Table 1 have been corrected, since R_y had not been considered by the other authors.

Comparing to Matos et al. (2015a), it is observed a high increase of the EE value when concentrated $W_1/O/W_2$ double emulsions are used, from 21.6% (at 20/80 volumetric ratio of W_1/O in W_2) to 77.5% (at 80/20 volumetric ratio of W_1/O in W_2).

Table 1. Characteristics and properties of different $W_1/O/W_2$ double emulsions formulated for encapsulating RSV

W_1	Oil	W_2	Initial RSV in W_1 (mg/L)	Surfactant W_1/O	Surfactant O/W_2	Ratio W_1/O	Ratio ($W_1/O/W_2$) (v/v)	EE (%)	RSV encapsulated in final double emulsion (mg/L)	Ref.
Ethanol/Water (20/80 v/v) + 0.1 M NaCl	Miglyol 812	Water + 0.1 M NaCl	50	PGPR	Tween 20	20:80	20/80	21.6[a]	0.43[d]	Matos et al., 2015a
Ethanol/Water (20/80 v/v) + 0.1 M NaCl	Miglyol 812	Water + 0.1 M NaCl	50	PGPR	Tween 20	20:80	80/20	77.5[b]	6.2[d]	Present work
Ethanol/Water (20/80 v/v) + 0.1 M NaCl	Canola oil	Water + 0.1 M NaCl + 0.5 wt % CMC	2500	PGPR	Whey proteins	20:80	40/60	98.0[c]	196[d]	Hemar et al., 2010
Pure water	Miglyol 812	Pure water	13.2	PGPR	Tween 80	20:80	20/80	94.97[c]	0.50[d]	Wang et al., 2017
Pure ethanol	Miglyol 812	Pure water	9703	PGPR	Tween 80	20:80	20/80	99.97[c]	388[d]	Wang et al., 2017

(a) 20% if the recovery yield (R_y) is taken into account
(b) 58.3% if R_y is taken into account
(c) Values taking into account R_y are not known
(d) Values calculated without taking into account R_y

RSV solubility at 20 °C: In water, 36 mg/L; In ethanol, 62,869 mg/L; In ethanol/water (20/80 v/v), 745 mg/L (Sun et al., 2008)

Although Hemar et al. (2010) did not report the EE of RSV in their original manuscript, we have calculated from the RSV present in both W_1 and W_2 aqueous phases that it should be as high as 98%. However, it is very important to point out that the initial amount of RSV in W_1 was extremely large what means that RSV was not completely dissolved under these conditions, as evidenced by the solubility values reported by Sun et al. (2008). Therefore, in these experiments, solid RSV had to be encapsulated and it could hardly be dissolved into W_2. In addition, as R_y was not calculated, an important overestimation of the EE value should be expected, making it not comparable to our results.

On the other hand, when our results are compared to those from Wang et al. (2017), it is evident that they reported larger values of EE using either pure water (94.97%) or pure ethanol (99.97%) as internal phase (W_1). However, if the concentration of RSV encapsulated in the final double emulsion is considered, we entrapped a higher amount of RSV using a 20/80 v/v of ethanol/water solution as W_1 (6.2 mg/L versus 0.50 mg/L when pure water was used). Wang et al. (2017) obtained the largest concentration of RSV (388 mg/L) when pure ethanol was used as W_1 phase. However, ethanol content needs to be controlled in food formulations.

3.4. Stability

The dispersed phase droplets of an emulsion (droplets of the W_1/O primary emulsion in this case) tend to migrate to the upper zone of the cell that contains the double emulsion. Several factors may influence the velocity of droplets migration such as continuous phase viscosity, densities of each phases, and mean diameter of dispersed phase droplets.

BS profiles are given in Fig. S1 (Supplementary Material). They show that the surfactant present in the external aqueous phase (W_2) prevents the coalescence of W_1/O droplets. However, a creaming process is observed in all cases, which is caused by the movement of the W_1/O droplets that tend to go to the upper part of the cell due to their lower density.

Fig. 4 shows the evolution of the thickness of the clarified layer for all double emulsions formulated without (Fig. 4A) and with (Fig. 4B) CMC in W_2. Although the emulsion samples were monitored for 9 days, only the evolution for the first 40 hours is given in Fig.4 as no changes were noticed afterwards.

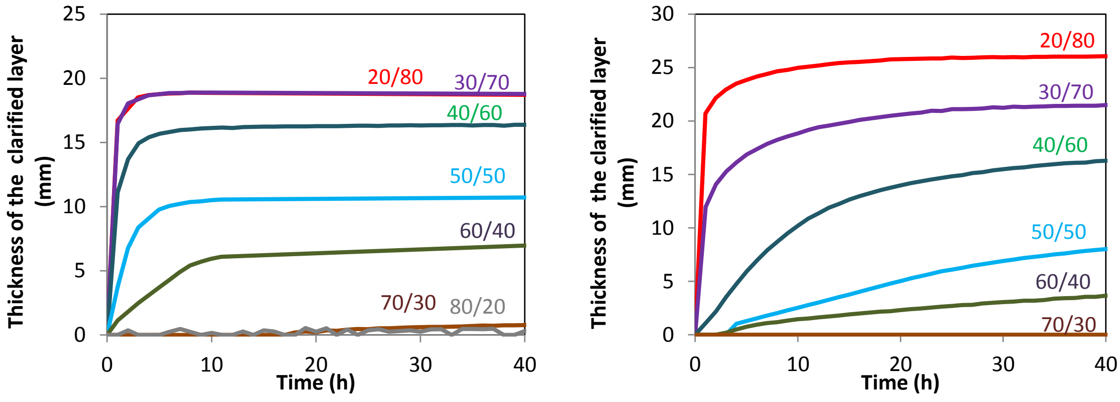

(A) (B)

Fig. 4. Thickness of the clarified layer vs time for $W_1/O/W_2$ double emulsions formulated at several volumetric ratios of W_1/O in W_2 without (A) and with (B) 0.5% (w/v) of CMC in the external aqueous phase

The creaming velocity decreased as the volumetric ratio of W_1/O in W_2 increased leading to more stable $W_1/O/W_2$ double emulsions, as it can be seen in Fig. 4. This is the expected behaviour, since the volume occupied by the W_1/O droplets is higher for high volumetric ratios and these droplets have less space to move what prevents creaming.

The clarified layer remained constant after the first few hours, especially for double emulsions with higher volumetric ratios. In addition, the thickness of the clarification layer for double emulsions without CMC (Fig. 4A) reached a constant value more quickly than those with CMC (Fig. 4B).

3.5. Rheology

Viscosity vs shear rate plots for all $W_1/O/W_2$ double emulsions are depicted in Fig. 5. Also shear stress vs shear rate graphs are given in Fig. S2 (Supplementary Material).

The flow properties of these double emulsions followed the Power Law or Oswalt-de Waele model (Eq. 3).

$$\sigma = K\,(\gamma)^n \tag{3}$$

where σ is the shear stress (Pa), γ is the shear rate (s^{-1}), K is the consistency index ($Pa{\cdot}s^n$), and n is the flow behaviour index (dimensionless).

This model has already been successfully applied to double emulsions with a 30/70 volumetric ratio of W_1/O in W_2 (Hernández-Marín et al., 2013).

Values of K and n for all the double emulsions prepared are summarized in Table 2.

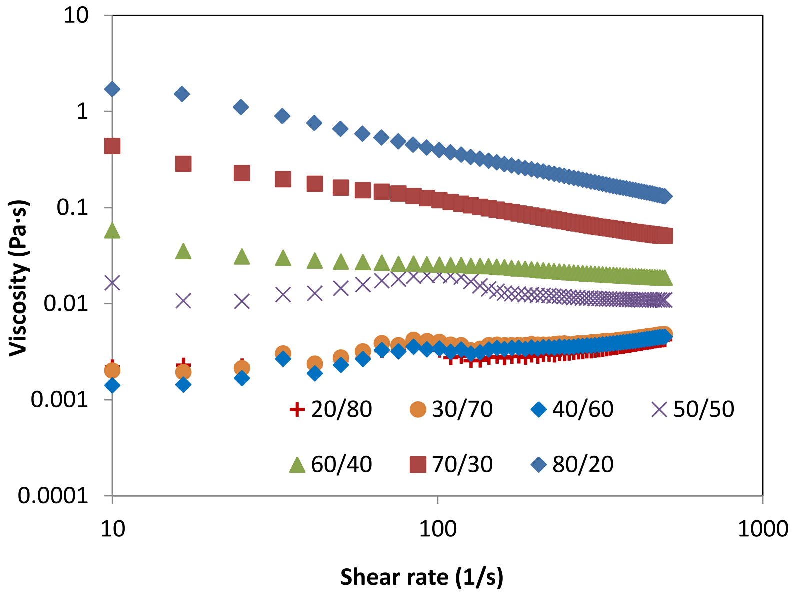

(A)

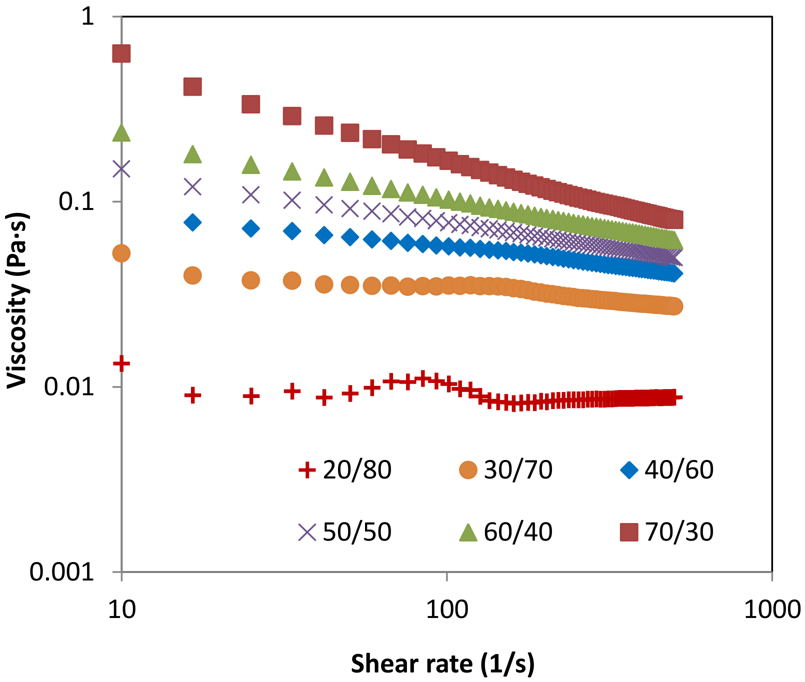

(B)

Fig. 5. Viscosity vs shear rate for $W_1/O/W_2$ double emulsions formulated at several volumetric ratios of W_1/O in W_2 without (A) and with (B) 0.5% (w/v) of CMC in the external aqueous phase

Table 2. Power law model parameters of $W_1/O/W_2$ double emulsions formulated at several volumetric ratios of W_1/O in W_2 without and with 0.5% (w/v) of CMC in the external aqueous phase

	Without CMC in W_2			With CMC in W_2		
W_1/O in W_2 (v/v)	K ($Pa \cdot s^n$)	n	R^2	K ($Pa \cdot s^n$)	n	R^2
20/80	0.0014	1.16	0.972	0.012	0.94	0.993
30/70	0.0021	1.12	0.972	0.063	0.87	0.998
40/60	0.0015	1.16	0.977	0.140	0.80	0.999
50/50	0.0022	0.86	0.996	0.607	0.66	0.999
60/40	0.066	0.79	0.996	0.540	0.67	0.999
70/30	1.28	0.48	0.998	2.55	0.48	0.997
80/20	10.5	0.29	0.997	-	-	-

Nearly all double emulsions behaved as pseudoplastic fluids with a more significant shear-thinning behaviour at lower n values. Only the double emulsion formulated with CMC at the lowest volumetric ratio (20/80) behaved almost as a Newtonian-like fluid. Similar results have been previously reported (Hernández-Marín et al., 2013; Matos et al., 2015a; O´Regan & Mulivhill, 2009; Yildrim et al., 2017). This shear-thinning behaviour is explained by the structural deformation of the network that is formed at equilibrium state. As higher shear stresses are applied, stronger elongations, network rupture, and deformation of droplets of primary emulsion occur, which leads to decrease apparent viscosity values (Yildrim et al., 2017).

Surprisingly, the double emulsions formulated without CMC at low volumetric ratios of W_1/O in W_2 (up to 40/60) showed a shear-thickening behaviour as values of n indicate. Experimental results in Fig. 5 show a viscosity peak approximately at the shear rate of 100 s^{-1}.

This unusual phenomenon had already been observed in highly concentrated surfactant solutions and it was attributed to shear-induced disordering and entanglement of the worm-like micelles of surfactant (Pal, 1992). It should be point out that double emulsions with less volume of W_1/O droplets contain larger amount of W_2

and hence more Tween 20 surfactant molecules. As the Tween 20 concentration is high and there is less oil/water interface to stabilize, worm-like micelles are more likely to appear.

The presence of CMC in the external aqueous phase seems to mitigate this effect, since it is just slightly observed for the lowest volumetric ratio of W_1/O in W_2. Small-amplitude oscillatory shear tests were performed to obtain mechanical spectra (Fig. 6 and 7) and, therefore, to ascertain whether viscous or elastic properties predominate in these double emulsions.

As shown in Fig. 6, both storage (G') and loss (G'') moduli had low values with marked dependence on frequency. Experimental data indicated an initial viscous behaviour where G'' was higher than G' until a crossover occurred ($G'(\omega_c) = G''(\omega_c)$) above a certain frequency, ω_c, of 2.5 rad/s for W_1/O/W_2 double emulsions formulated without CMC at volumetric ratios of W_1/O in W_2 in the range 20/80 – 60/40 (Fig. 6A-6B). Beyond this point, G' was higher than G'' for the frequency range covered. Therefore, the viscoelastic behaviour of double emulsions formulated at low volumetric ratios corresponds to complex or polymeric solutions, where G' and G'' curves intersect within the range of tested frequencies, which indicates a clear fluid-like behaviour.

In contrast, W_1/O/W_2 double emulsions formulated at 70/30 and 80/20 volumetric ratios of W_1/O in W_2 show a dominant elastic character (G' is higher than G'' for all the frequency range in Fig. 6B).

This unusual bulk elasticity showed by the most concentrated W_1/O/W_2 double emulsions had been already reported for highly concentrated simple emulsions stabilized with proteins (Dimitrova & Leal-Calderón, 2004).

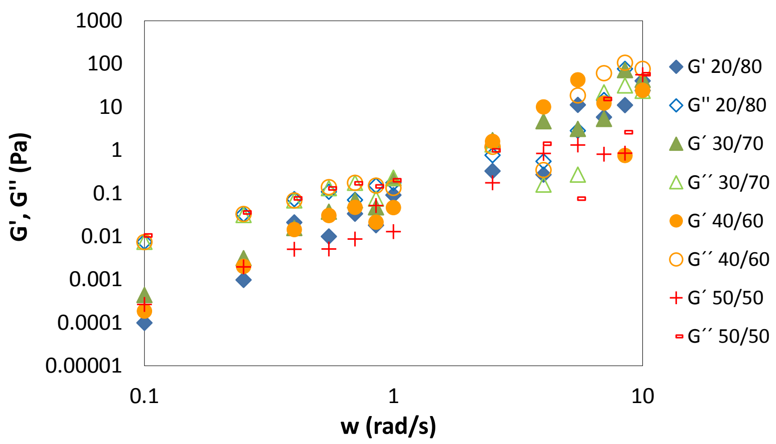

(A)

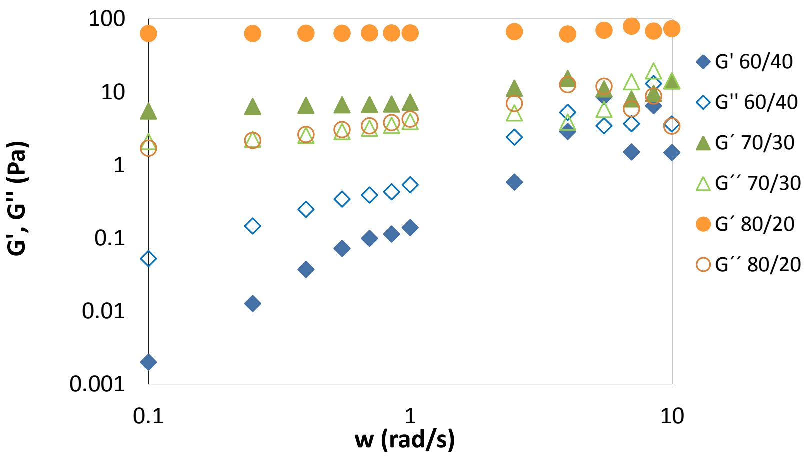

(B)

Fig. 6. Storage (G´) and loss (G´´) moduli vs frequency for $W_1/O/W_2$ double emulsions formulated without CMC in the external aqueous phase at several volumetric ratios of W_1/O in W_2: (A) 20/80, 30/70, 40/60, 50/50; (B) 60/40, 70/30, 80/20

A similar trend was found for $W_1/O/W_2$ double emulsions formulated with CMC in W_2 (Fig. 7), but the change of rheological behaviour appeared at lower volumetric ratios. Therefore, it was observed an initial viscous behaviour where G" was higher than G' until a crossover occurred around 4 rad/s for $W_1/O/W_2$ double emulsions formulated with CMC at volumetric ratios of W_1/O in W_2 in the range 20/80 – 40/60 (Fig.7A). A dominant elastic character was observed for volumetric ratios ranging from 50/50 to 70/30 (Fig. 7A-7B).

Results previously reported for diluted double emulsions (up to 30/70 volumetric ratio of W_1/O in W_2) (Keyvani et al., 2014) showed a viscous behaviour for all the frequency ranged covered. It is important to point out that those double emulsions did not have thickening agent in the external aqueous phase, as it is the case of the emulsions formulated without CMC in the present study.

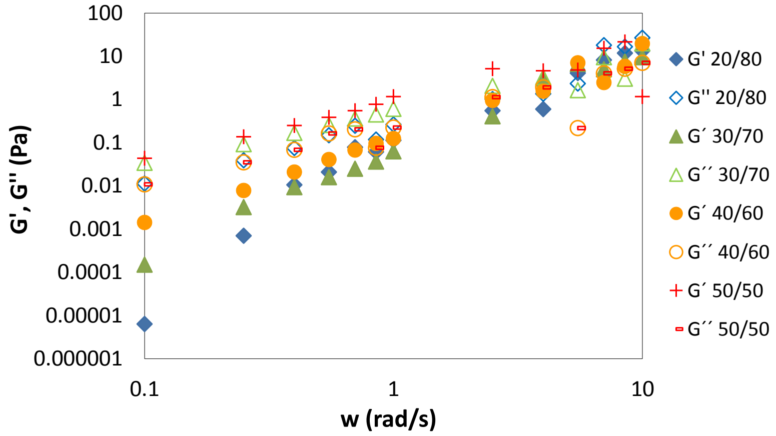

(A)

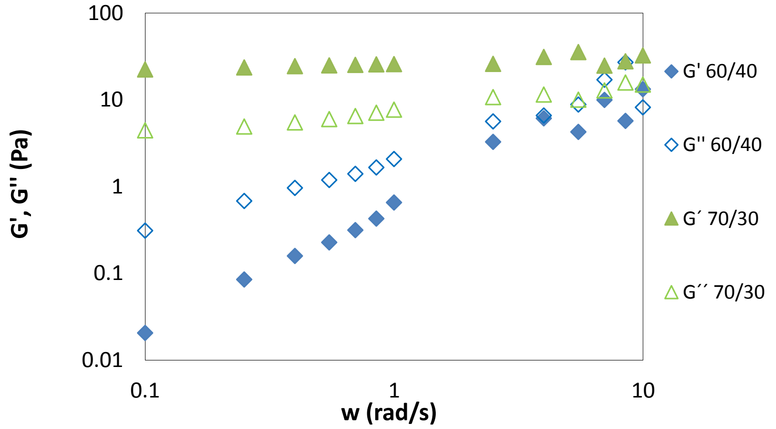

(B)

Fig. 7. Storage (G´) and loss (G´´) moduli vs frequency for $W_1/O/W_2$ double emulsions formulated with 5% (w/v) CMC in the external aqueous phase at several volumetric ratios of W_1/O in W_2: (A) 20/80, 30/70, 40/60, 50/50; (B) 60/40, 70/30

4. Conclusions

In this work, concentrated $W_1/O/W_2$ double emulsions containing RSV were prepared by a conventional two-step mechanical emulsification process, which could be appropriate for the double emulsions production on an industrial scale. Moreover, these concentrated double emulsions (with 6.2 mg/L of encapsulated RSV) showed high encapsulation efficiency (up to 58%), good storage stability, shear-thinning behaviour, and dominant elastic character, which makes them suitable for food applications.

Once this food application is selected, it would be necessary further work to explore the incorporation of RSV-entrapped double emulsion into the final product. The impact of food matrices on the stability and controlled delivery of RSV should be especially undertaken, as well as the effects of the concentrated double emulsions on the physicochemical, rheological and sensory properties of this final product.

Funding

This study was financed by the Consejería de Economía y Empleo del Principado de Asturias (Plan de Ciencia, Tecnología e Innovación 2013-2017) through the Grant GRUPIN14-022. Support from the European Regional Development Fund (ERDF) is also gratefully acknowledged.

References

Amri, A., Chaumeil, J.C., Sfar, S., & Charreau, C. (2012). Administration of resveratrol: What formulation solutions to bioavailability limitations?. *Journal of Controlled Release,* 158, 182-193.

Aserin, A. (2008). *Multiple emulsions: Technology and applications*, Wiley Interscience, Hoboken, N.J.

Babak, V.G., & Stebe, M.J. (2002). Highly concentrated emulsions: Physicochemical principles of formulation. *Journal of Dispersion Science and Technology,* 23, 1-22.

Cameron, N.R., & Sherrington, D.C. (1996). High internal phase emulsions (HIPEs) - Structure, properties and use in polymer preparation. In *Biopolymers Liquid Crystalline Polymers Phase Emulsion*. *Advances in Polymer Science,* 126, 163-214.

Davidov-Pardo, G., & McClements, D.J. (2014). Resveratrol encapsulation: Designing delivery systems to overcome solubility, stability and bioavailability issues. *Trends in Food Science and Technology,* 38, 88-103.

Diaz-Gerevine, G.T., Repossi, G., Dain, A., Tarres, M.C., Das, U.N., & Eynard, A.R. (2016). Beneficial action of resveratrol: How and why?. *Nutrition,* 32, 174-178.

Dimitrova, T.D., & Leal-Calderon, F. (2004). Rheological properties of highly concentrated protein-stabilized emulsions. *Advances in Colloid and Interface Science,* 108, 49-61.

Francioso, A., Mastromarino, P., Masci, A., d'Erme, M., & Mosca, L. (2014). Chemistry, stability and bioavailability of resveratrol. *Medicinal Chemistry,* 10, 237-245.

Ganesan, P., & Choi, D.K. (2016). Current application of phytocompound-based nanocosmeceuticals for beauty and skin therapy. *International Journal of Nanomedicine,* 11, 1987-2007.

Garti, N. (1997). Progress in stabilization and transport phenomena of double emulsions in food applications. *LWT-Food Science and Technology,* 30, 222-235.

Gomes-Silva, C., Monteiro, J., Marques, R.R.N., Silva, A.M.T., Martínez, C., Canle, M., & Faria, J.L. (2013). Photochemical and photocatalytic degradation of trans-resveratrol. *Photochemical & Photobiological Sciences,* 12, 638–644.

Guerrero, R.F., García-Parrilla, M.C., Puertas, B., & Cantos-Villar, E. (2009). Wine, resveratrol and health: a review. *Natural Product Communications,* 4, 635-658.

Gutiérrez, G., Matos, M., Benito, J.M., Coca, J., & Pazos, C. (2014). Preparation of HIPEs with controlled droplet size containing lutein. *Colloids and Surfaces A: Physicochemical and Engineering Aspects,* 442, 69-79.

Hemar, Y., Cheng, L.J., Oliver, C.M., Sanguansri, L., & Augustin, M. (2010). Encapsulation of resveratrol using water-in-oil-in-water double emulsions. *Food Biophysics,* 5, 120-127.

Hernández-Marín, N.Y., Lobato-Calleros, C., & Vernon-Carter, E.J. (2013). Stability and rheology of water-in-oil-in-water multiple emulsions made with protein-polysaccharide soluble complexes. *Journal of Food Engineering,* 119, 181-187.

Jiang, J., Mei, Z., Xu, J., & Sun, D. (2013). Effect of inorganic electrolytes on the formation and stability of water-in-oil (W/O) emulsions. *Colloids and Surfaces A: Physicochemical and Engineering Aspects,* 429, 82-90.

Keyvani, M., Davarpanah, L., & Vahabzadeh, F. (2014). Rheological characterization of ferrous sulfate-containing water-in-oil-in-water ($W_1/O/W_2$) double emulsions. *Korean Journal of Chemical Engineering,* 31, 1681-1694.

Kim, J-W., Kang, H-H., Suh, K-D., & Oh, S-G. (2003). Stabilization of water-soluble antioxidant in water-in-oil-in-water double emulsion. *Journal of Dispersion Science and Technology,* 24, 833-839.

Leal-Calderon, F., Homer, S., Goh, A., & Lundin, L. (2012). W/O/W emulsions with high internal droplet volume fraction. *Food Hydrocolloids,* 27, 30-41.

Lei, L., Zhang, Q., Shi, S., & Zhu, S. (2016). High internal phase emulsion with double emulsion morphology and their templated porous polymer systems. *Journal of Colloid and Interface Science,* 483, 232-240.

Li, Z., Liu, H.R., Zeng, L., Liu, H.W., Yang, S., & Wang, Y.M. (2014). Preparation of high internal water-phase double emulsions stabilized by a single anionic surfactant for fabricating interconnecting porous polymer microspheres. *Langmuir,* 30, 12154-12163.

Llinàs, M., Calderó, G., García-Celma, M.J., Patti, A., & Solans, C. (2013). New insights on the mechanisms of drug release from highly concentrated emulsions. *Journal of Colloid and Interface Science,* 394, 337-345.

Márquez, A.L., Medrano, A., Panizzolo, L.A., & Wagner, J.R. (2010). Effect of calcium salts and surfactant concentration on the stability of water-in-oil emulsions prepared with polyglycerol polyricinoleate. *Journal of Colloid and Interface Science,* 341, 101-108.

Matos, M., Gutiérrez, G., Coca, J., & Pazos, C. (2014). Preparation of water-in-oil-in-water ($W_1/O/W_2$) double emulsions containing resveratrol. *Colloids and Surfaces A: Physicochemical and Engineering Aspects,* 442, 111-122.

Matos, M., Gutiérrez, G., Iglesias, O., Coca, J., & Pazos, C. (2015a). Enhancing encapsulation efficiency of food-grade double emulsions containing resveratrol or vitamin B_{12} by membrane emulsification. *Journal of Food Engineering,* 166, 212–220.

Matos, M., Gutiérrez, G., Iglesias, O., Coca, J., & Pazos, C. (2015b). Characterization, stability and rheology of highly concentrated monodisperse emulsions containing lutein. *Food Hydrocolloids,* 49, 156–163.

McClements, D.J., & Li, Y. (2010). Structured emulsion-based delivery systems controlling the digestion and release of lipophilic food components. *Advances in Colloid and Interface Science,* 159, 213-228.

Mullin, G.E. (2011). Red wine, grapes, and better health – Resveratrol. *Nutrition in Clinical Practice,* 26, 722-723.

Murtaza, G., Latif, U., Najam-Ul-Haq, M., Sajjad, A., Karim, S., Akhtar, M.,& Hussain, I. (2013). Resveratrol: An active natural compound in red wines for health. *Journal of Food and Drug Analysis,* 21, 1-12.

Muschiolik, G. (2007). Multiple emulsions for food use. *Current Opinion in Colloid & Interface Science,* 12, 213–220.

Muschiolik, G., & Dickinson, E. (2017). Double emulsions relevant to food systems: Preparation, stability, and applications. *Comprehensive Reviews in Food Science and Food Safety,* 16, 532-555.

Neves, A.R., Lúcio, M., Lima, J.L.C., & Reis, S. (2012). Resveratrol in medicinal chemistry: A critical review of its pharmacokinetics, drug-delivery, and membrane interaction. *Current Medicinal Chemistry,* 19, 1663-1681.

Novelle, M.G., Wahl, D., Diéguez, C., Bernier, M., & de Cabo, R. (2015). Resveratrol supplementation: Where are we now and where should we go?. *Ageing Research Reviews,* 21, 1-15.

O´Regan, J., & Mulivhill, D.M. (2009). Water soluble inner aqueous phase markers as indicators of the encapsulation properties of water-in-oil-in-water emulsions stabilized with sodium caseinate. *Food Hydrocolloids,* 23, 2339-2345.

Pal, R. (1992). Rheological behaviour of concentrated surfactant solutions and emulsions. *Colloids and Surfaces,* 64, 207-215.

Pal, R. (2011). Rheology of simple and multiple emulsions. *Current Opinion in Colloid & Interface Science,* 16, 41-60.

Pangeni, P., Sahni, J., Ali, J., Sharma, S., & Baboota, S. (2014). Resveratrol: Review on therapeutic potential and recent advances in drug delivery. *Expert Opinion on Drug Delivery,* 11, 1285-1298.

Park, C.I., Cho, W.G., & Lee, S.J. (2003). Emulsion stability of cosmetic creams based on water-in-oil high internal phase emulsions. *Korea-Australia Rheology Journal,* 15, 125-130.

Rondón-González, M., Sadtler, V., Choplin, L., & Salager, J.L. (2006). Emulsion catastrophic inversion from abnormal to normal morphology. 5. Effect of the water-to-oil ratio and surfactant concentration on the inversion produced by continuous stirring. *Industrial and Engineering Chemistry Research,* 45, 3074–3080.

Saiko, P., Szakmary, A., Jaeger, W., & Szekeres, T. (2008). Resveratrol and its analogs: Defense against cancer, coronary disease and neurodegenerative maladies or just a fad?, *Mutation Research-Reviews in Mutation Research,* 658, 68-94.

Schuch, A., Deiters, P., Henne, J., Köhler, K., & Schuchmann, H.P. (2013). Production of W/O/W (water-in-oil-in-water) multiple emulsions: droplet breakup and release of water. *Journal of Colloid and Interface Science,* 402, 157-164.

Sessa, M., Balestrieri, M.L., Ferrari, G., Servillo, L., Castaldo, D., D'Onofrio, N., Donsi, F., & Tsao, R. (2014). Bioavailability of encapsulated resveratrol into nanoemulsion-based delivery systems. *Food Chemistry,* 147, 42-50.

Silverstein, M.S. (2014). PolyHIPEs: Recent advances in emulsion-templated porous polymers. *Progress in Polymer Science,* 39,199-234.

Solans, C., Esquena,J., & Azemar, N. (2003). Highly concentrated (gel) emulsions, versatile reaction media. *Current Opinion in Colloid & Interface Science,* 8, 156-163.

Soo, E., Thakur, S., Qu, Z., Jambhrunkar, S., & Parekh, H.S. (2016). Enhancing delivery and cytotoxicity of resveratrol through a dual nanoencapsulation approach. *Journal of Colloid and Interface Science,* 462, 368-374.

Summerlin, N., Soo, E., Thakur, S., Qu, Z., Jambhrunkar, S., & Popat, A. (2015). Resveratrol nanoformulations: Challenges and opportunities. *International Journal of Pharmaceutics,* 479, 282-290.

Sun, X., Shao, Y., & Yan, W. (2008). Measurement and correlation of solubilities of trans-resveratrol in ethanol + water and acetone + water mixed solvents at different temperatures. *Journal of Chemical & Engineering Data,* 53, 2562–2566.

Wang, J., Shi, A., Agyei, D., & Wang, Q. (2017). Formulation of water-in-oil-in-water (W/O/W) emulsions containing trans-resveratrol. *RSC Advances*, 7, 35917-35927.

Wolf, F., Koehler, L., & Schuchmann, H.P. (2013). Stabilization of water droplets in oil with PGPR for use in oral and dermal applications. *Journal of Food Processing Engineering,* 36, 276-283.

Yang, T., Wang, L., Zhu, M., Zhang, L., & Yan, L. (2015). Properties and molecular mechanisms of resveratrol: a review*. Pharmazie,* 70, 501-506.

Yang, X., Li, X., & Ren, J. (2014). From French paradox to cancer treatment: Anti-cancer activities and mechanisms of resveratrol. *Anti-Cancer Agents in Medicinal Chemistry,* 14, 806–825.

Yildrim, M., Summu, G., & Sahin, S. (2017).The effects of emulsifier type, phase ratio, and homogenization methods on stability of the double emulsion, *Journal of Dispersion Science and Technology,* 38, 807-814.

Zhang, T., & Guo, Q. (2017). Continuous preparation of polyHIPE monoliths from ionomer-stabilized high internal phase *emulsions* (*HIPEs*) for efficient recovery of spilled oils. *Chemical Engineering Journal*, 307, 812-819.

Figure captions

Fig. 1. Droplet size distributions of the W_1O primary emulsion (A) and the $W_1/O/W_2$ double emulsions formulated at several volumetric ratios of W_1/O in W_2 without (B) and with (C) 0.5% (w/v) of CMC in the external aqueous phase

Fig. 2. Optical microscopy images of $W_1/O/W_2$ double emulsions formulated without and with 0.5% (w/v) of CMC in W_2 at several volumetric ratios of W_1/O in W_2

Fig. 3. Encapsulation efficiency of RSV for $W_1/O/W_2$ double emulsions formulated without and with 0.5% (w/v) of CMC in the external aqueous phase at several volumetric ratios of W_1/O in W_2

Fig. 4. Thickness of the clarified layer vs time for $W_1/O/W_2$ double emulsions formulated at several volumetric ratios of W_1/O in W_2 without (A) and with (B) 0.5% (w/v) of CMC in the external aqueous phase

Fig. 5. Viscosity vs shear rate for $W_1/O/W_2$ double emulsions formulated at several volumetric ratios of W_1/O in W_2 without (A) and with (B) 0.5% (w/v) of CMC in the external aqueous phase

Fig. 6. Storage (G´) and loss (G´´) moduli vs frequency for $W_1/O/W_2$ double emulsions formulated without CMC in the external aqueous phase at several volumetric ratios of W_1/O in W_2: (A) 20/80, 30/70, 40/60, 50/50; (B) 60/40, 70/30, 80/20

Fig. 7. Storage (G´) and loss (G´´) moduli vs frequency for $W_1/O/W_2$ double emulsions formulated with 5% (w/v) CMC in the external aqueous phase at several volumetric ratios of W_1/O in W_2: (A) 20/80, 30/70, 40/60, 50/50; (B) 60/40, 70/30

Figure 1 colour

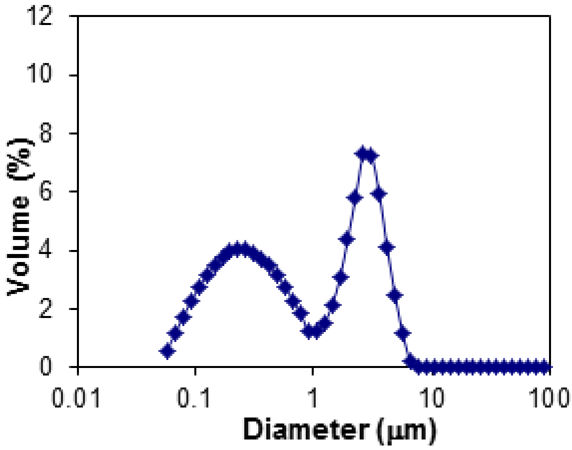

(A)

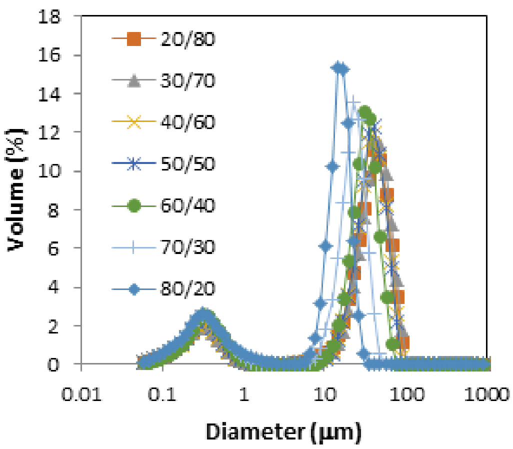

(B)

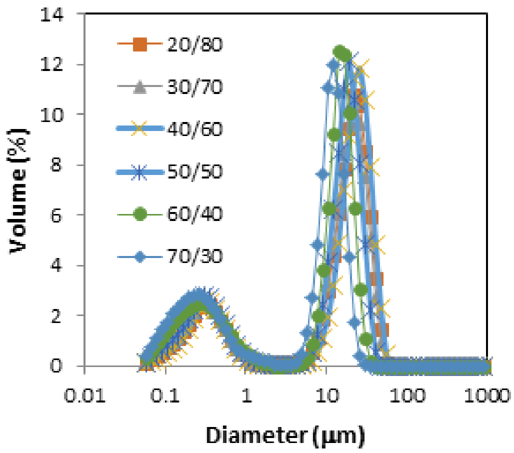

(C)

Figure 1

Figure 1 b&w

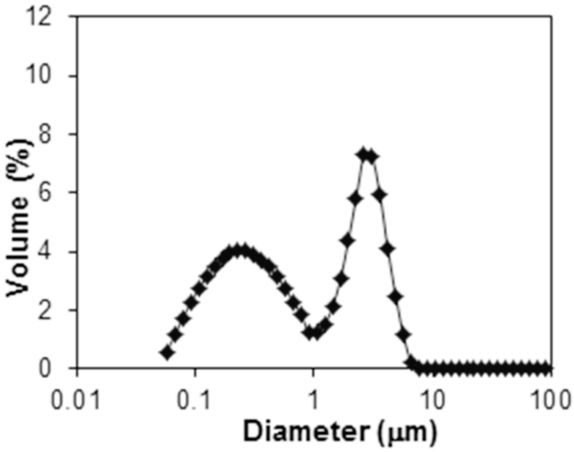

(A)

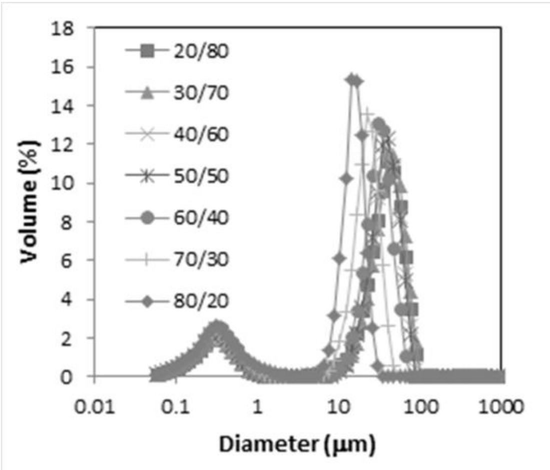

(B)

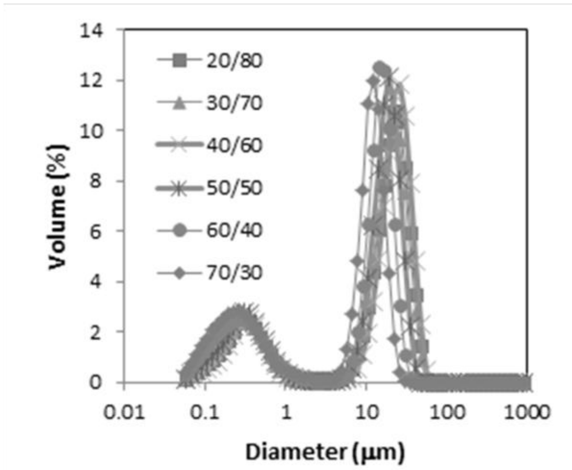

(C)

Figure 1

Figure 2

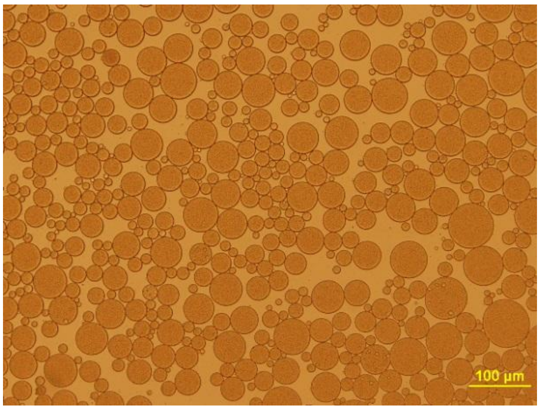

30/70 without CMC in W_2

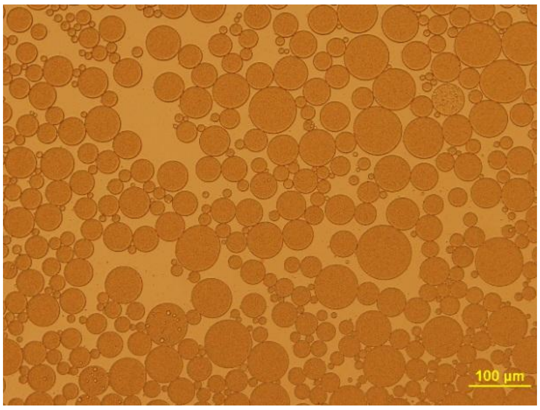

30/70 with CMC in W_2

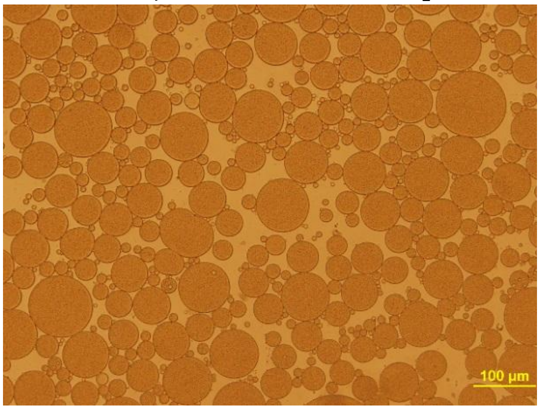

50/50 without CMC in W_2

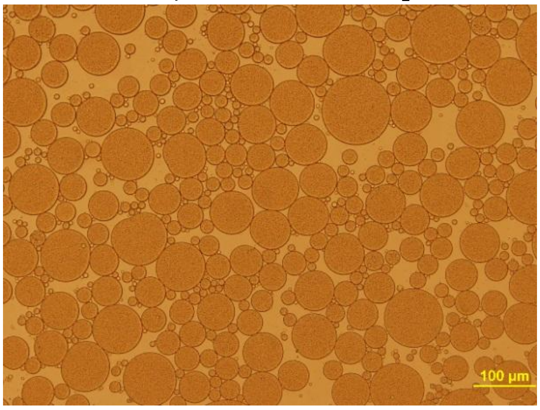

50/50 with CMC in W_2

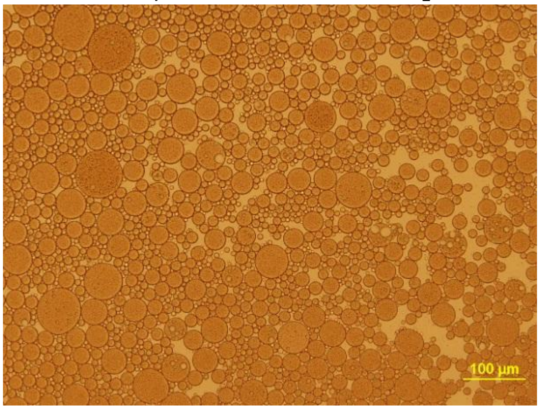

70/30 without CMC in W_2

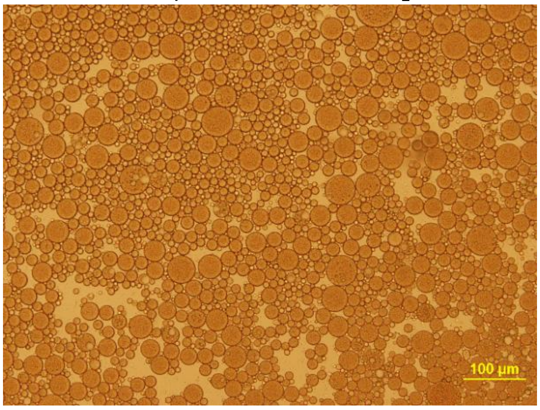

70/30 with CMC in W_2

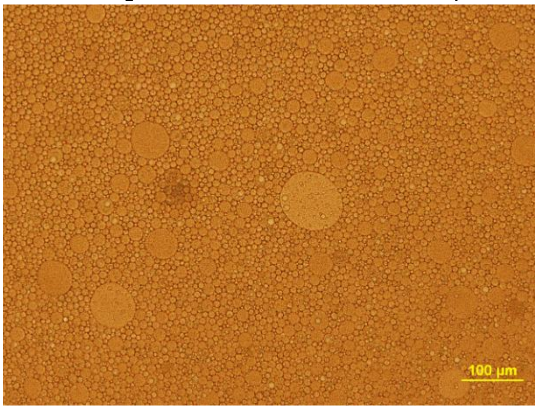

80/20 without CMC in W_2

Figure 2

Figure 3 colour

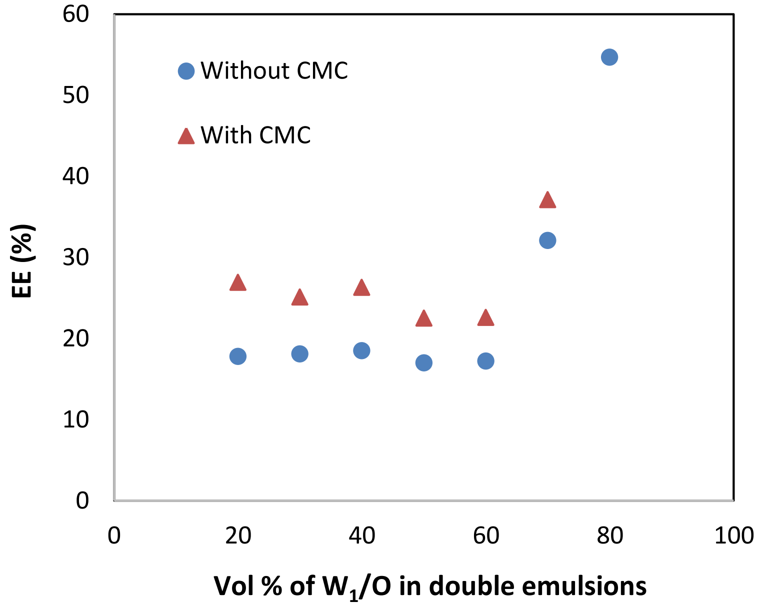

Figure 3

Figure 3 b&w

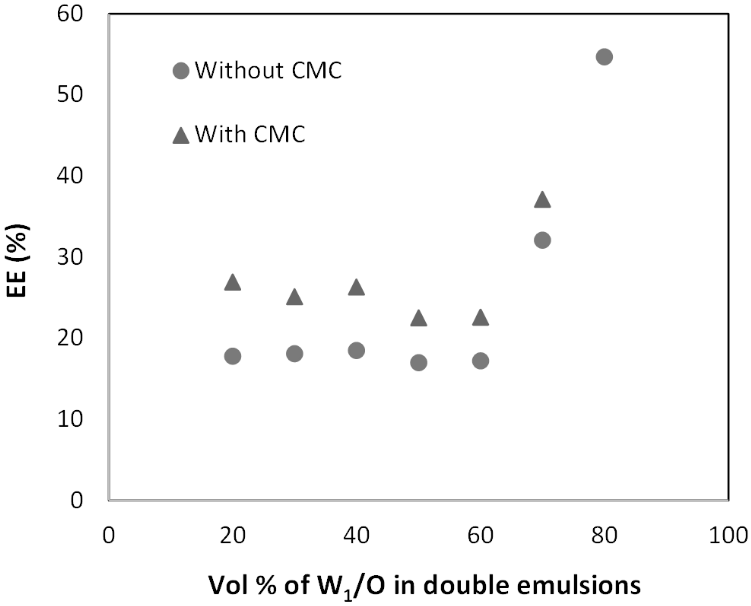

Figure 3

Figure 4 colour

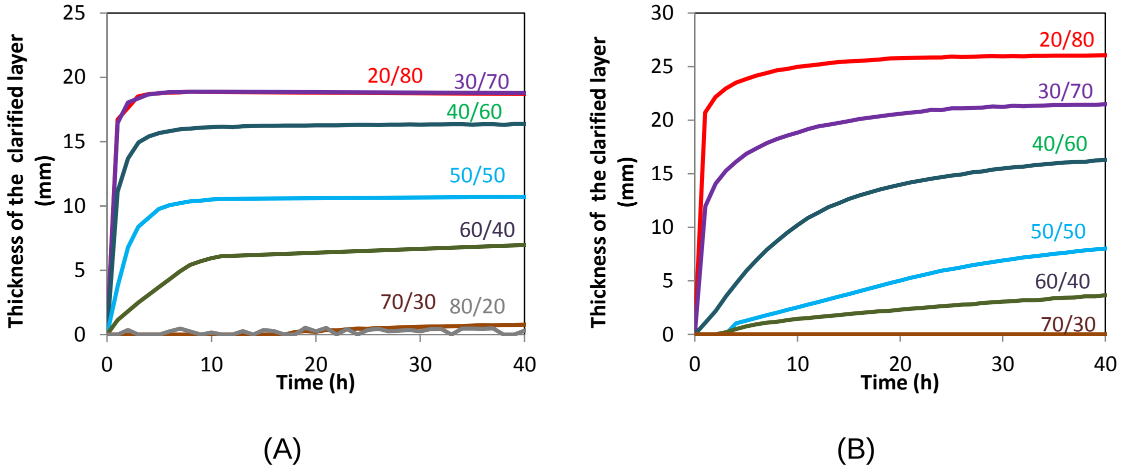

Figure 4

Figure 4 b&w

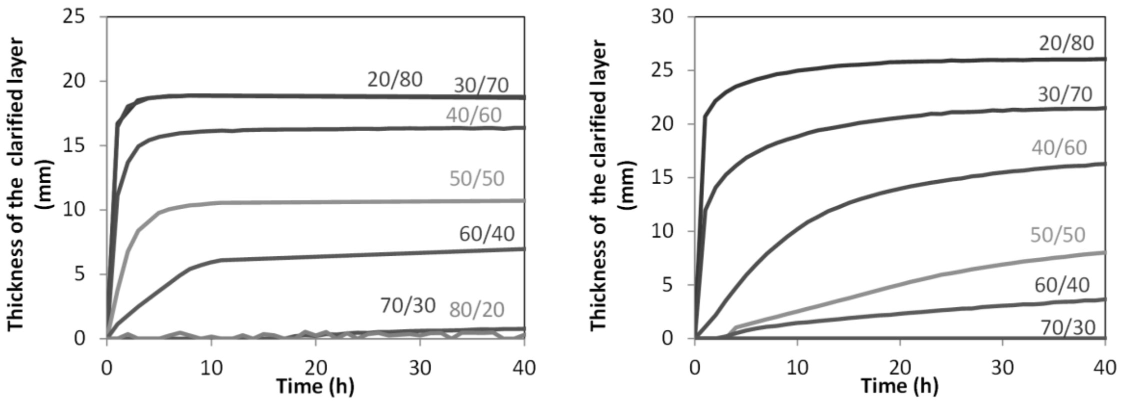

(A) (B)

Figure 4

Figure 5 colour

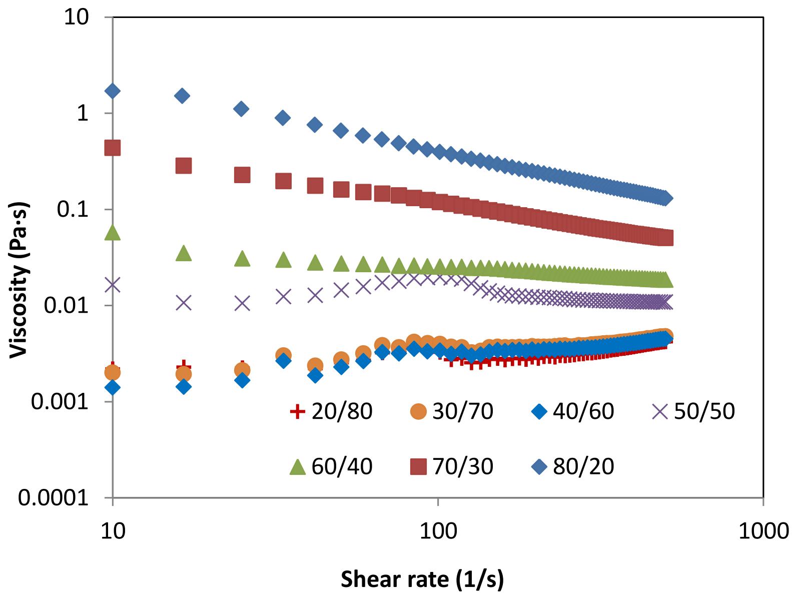

(A)

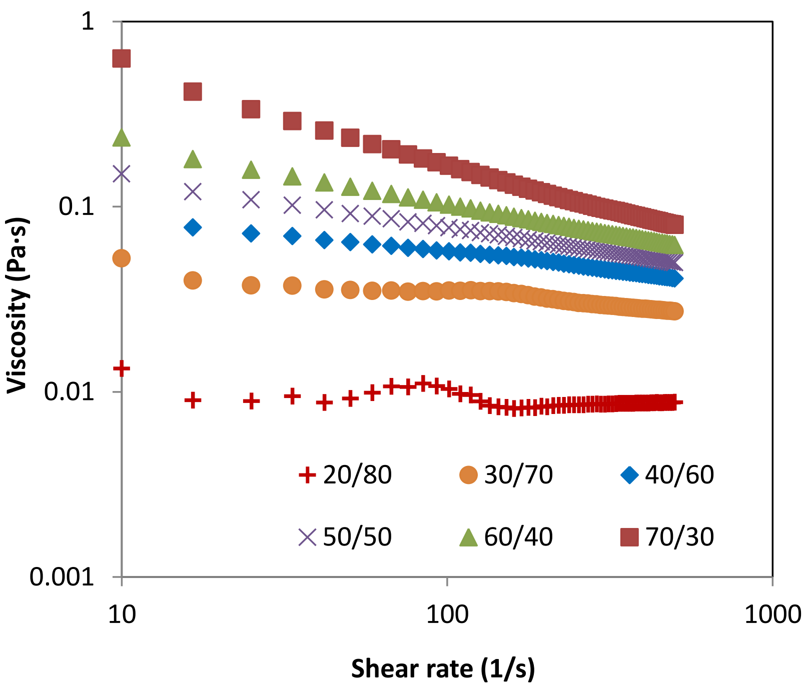

(B)

Figure 5

Figure 5 b&w

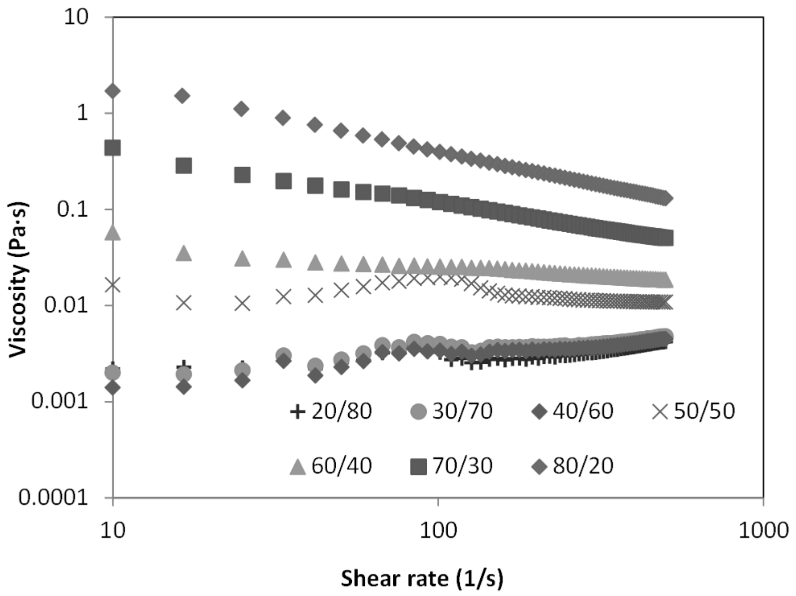

(A)

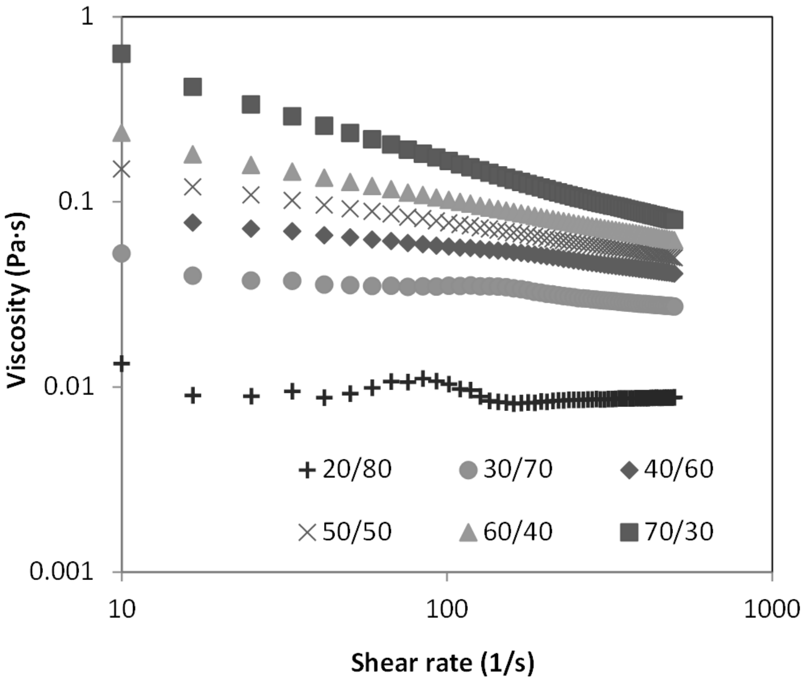

(B)

Figure 5

Figure 6 colour

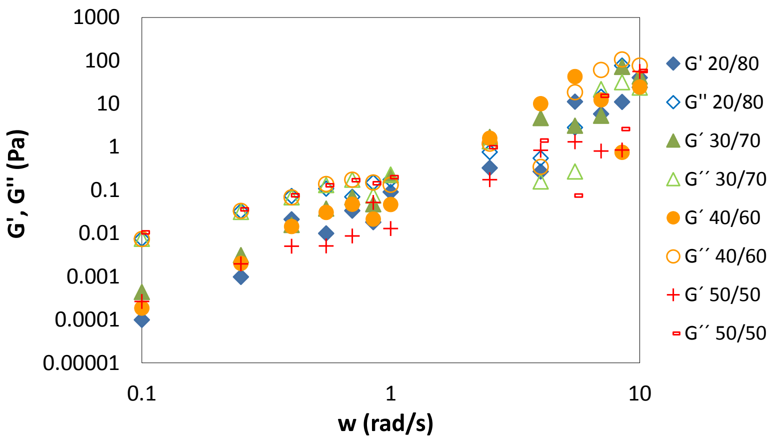

(A)

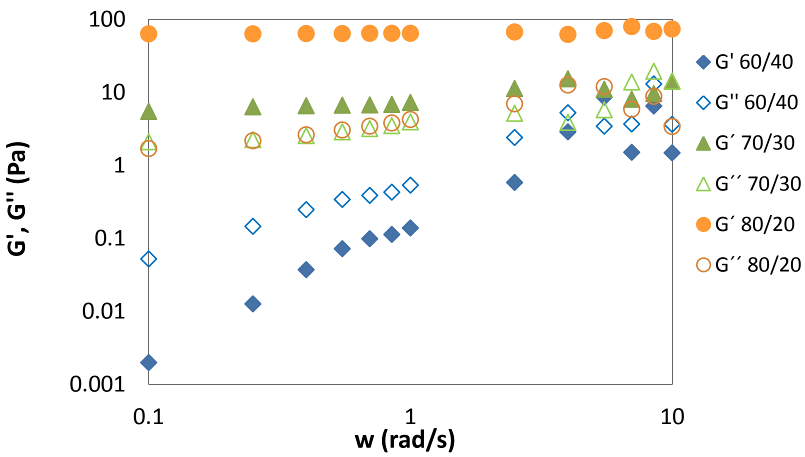

(B)

Figure 6

Figure 6 b&w

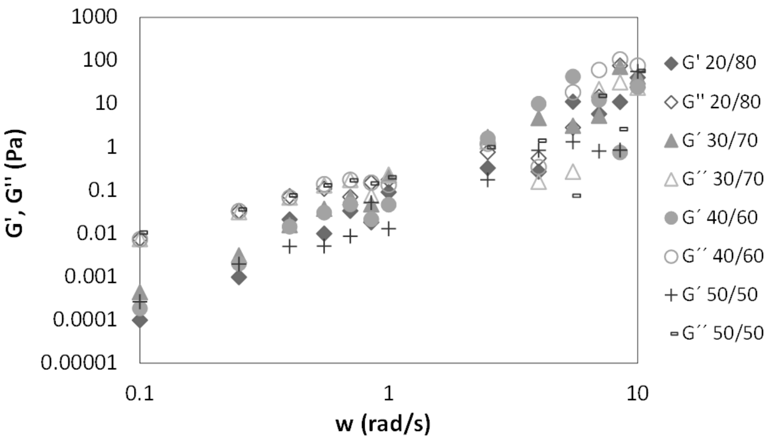

(A)

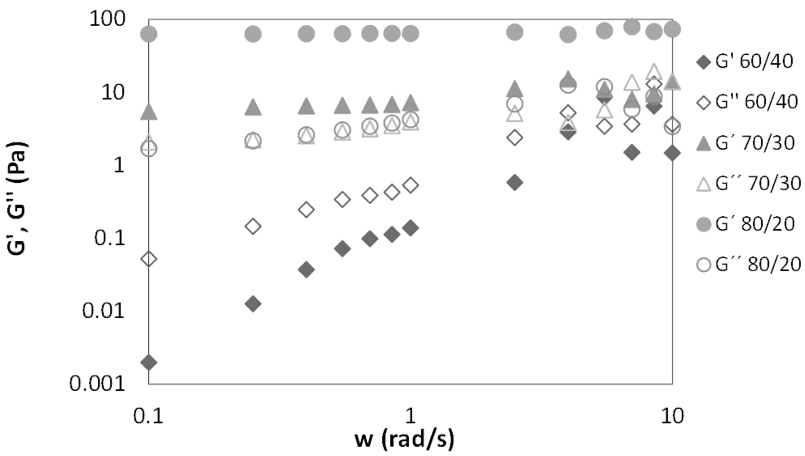

(B)

Figure 6

Figure 7 colour

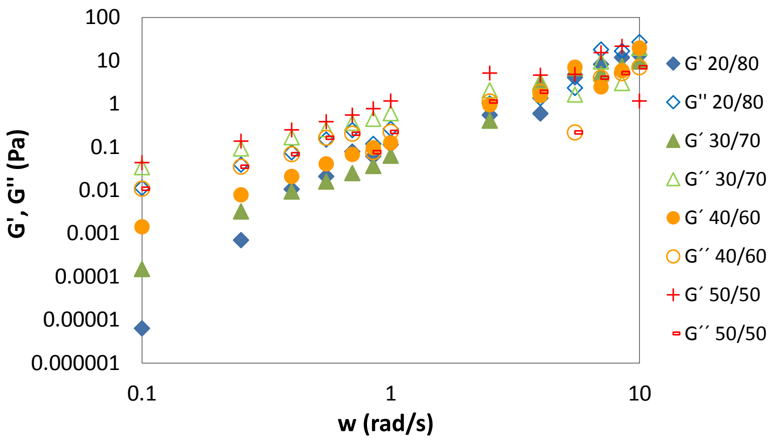

(A)

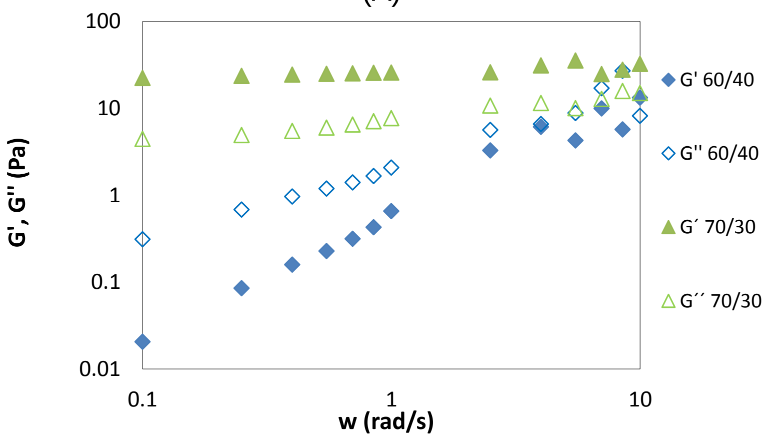

(B)

Figure 7

Figure 7 b&w

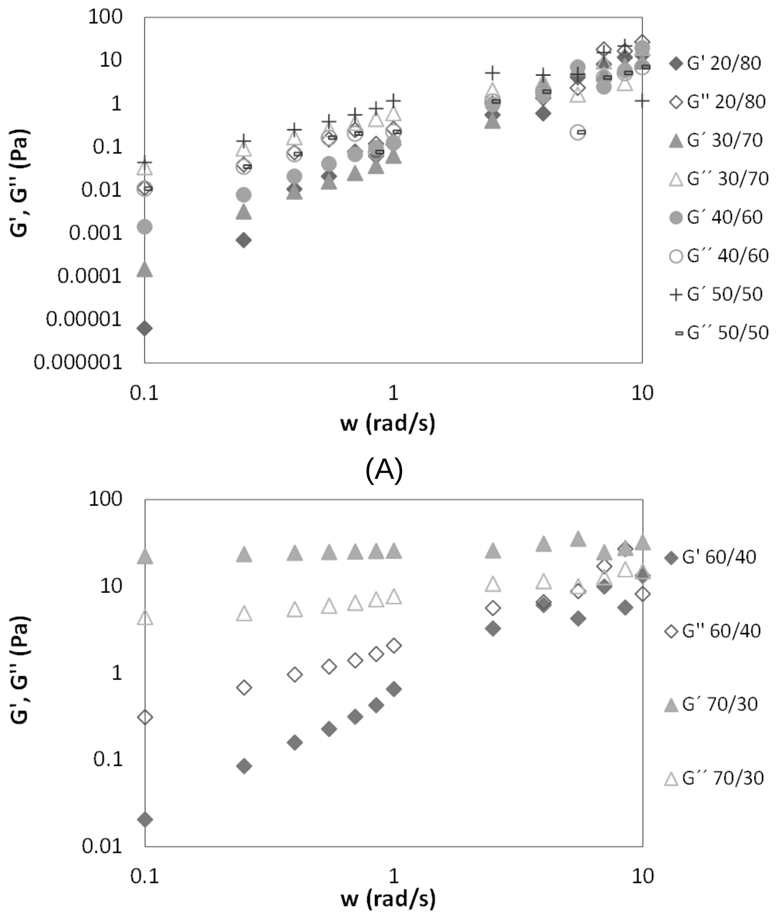

(A)

(B)

Figure 7

Table 1

Table 1. Characteristics and properties of different $W_1/O/W_2$ double emulsions formulated for encapsulating RSV

W_1	Oil	W_2	Initial RSV in W_1 (mg/L)	Surfactant W_1/O	Surfactant O/W_2	Ratio W_1/O	Ratio ($W_1/O/W_2$ (v/v)	EE (%)	RSV encapsulated in final double emulsion (mg/L)	Ref.
Ethanol/Water (20/80 v/v) + 0.1 M NaCl	Miglyol 812	Water + 0.1 M NaCl	50	PGPR	Tween 20	20:80	20/80	21.6[a]	0.43[d]	Matos et al., 2015a
Ethanol/Water (20/80 v/v) + 0.1 M NaCl	Miglyol 812	Water + 0.1 M NaCl	50	PGPR	Tween 20	20:80	80/20	77.5[b]	6.2[d]	Present work
Ethanol/Water (20/80 v/v) + 0.1 M NaCl	Canola oil	Water + 0.1 M NaCl + 0.5 wt % CMC	2500	PGPR	Whey proteins	20:80	40/60	98.0[c]	196[d]	Hemar et al., 2010
Pure water	Miglyol 812	Pure water	13.2	PGPR	Tween 80	20:80	20/80	94.97[c]	0.50[d]	Wang et al., 2017
Pure ethanol	Miglyol 812	Pure water	9703	PGPR	Tween 80	20:80	20/80	99.97[c]	388[d]	Wang et al., 2017

(a) 20% if the recovery yield (R_y) is taken into account

(b) 58.3% if R_y is taken into account

(c) Values taking into account R_y are not known

(d) Values calculated without taking into account R_y

RSV solubility at 20 ^oC: In water, 36 mg/L; In ethanol, 62,869 mg/L; In ethanol/water (20/80 v/v), 745 mg/L (Sun et al., 2008)

Table 2

Table 2. Power law model parameters of $W_1/O/W_2$ double emulsions formulated at several volumetric ratios of W_1/O in W_2 without and with 0.5% (w/v) of CMC in the external aqueous phase

	Without CMC in W_2			With CMC in W_2		
W_1/O in W_2 (v/v)	K ($Pa\cdot s^n$)	n	R^2	K ($Pa\cdot s^n$)	n	R^2
20/80	0.0014	1.16	0.972	0.012	0.94	0.993
30/70	0.0021	1.12	0.972	0.063	0.87	0.998
40/60	0.0015	1.16	0.977	0.140	0.80	0.999
50/50	0.0022	0.86	0.996	0.607	0.66	0.999
60/40	0.066	0.79	0.996	0.540	0.67	0.999
70/30	1.28	0.48	0.998	2.55	0.48	0.997
80/20	10.5	0.29	0.997	-	-	-

Supplementary Interactive Plot Data (CSV)
Click here to download Supplementary Interactive Plot Data (CSV): Supplementary Material revised.docx